A unifying scaling theory for vortex dynamics in two-dimensional turbulence

D. G. Dritschel[1], R. K. Scott[1], C. Macaskill[2], G. A. Gottwald[2] and C. V. Tran[1]

[1]*School of Mathematics and Statistics,*

University of St Andrews, St Andrews KY16 9SS, UK

e-mail: dgd@mcs.st-and.ac.uk, chuong@mcs.st-and.ac.uk, rks@mcs.st-and.ac.uk

[2]*School of Mathematics and Statistics,*

University of Sydney, NSW 2006, Australia

e-mail: charlie@maths.usyd.edu.au, gottwald@maths.usyd.edu.au

Abstract

We present a scaling theory for unforced inviscid two-dimensional turbulence. Our model unifies existing spatial and temporal scaling theories. The theory is based on a self-similar distribution of vortices of different sizes A. Our model uniquely determines the spatial and temporal scaling of the associated vortex number density which allows the determination of the energy spectra and the vortex distributions. We find that the vortex number density scales as $n(A,t) \sim t^{-2/3}/A$, which implies an energy spectrum $\mathcal{E} \sim k^{-5}$, significantly steeper than the classical Batchelor-Kraichnan scaling. High-resolution numerical simulations corroborate the model.

PACS numbers: 47.27.-i

Keywords: two-dimensional turbulence, vortex dynamics

There has been a renewed interest in two-dimensional turbulence in recent years, motivated by its applicability as a simple model for large-scale geophysical flows. The earth's atmosphere has an approximate two-dimensional structure, as the troposphere is only approximately 10km deep, while the horizontal extension is more than $40,000$km. Moreover, the fast rotation of the earth leads to a vertical alignment enhancing the two-dimensional character of large-scale dynamics. As a result, two-dimensional turbulence has been regarded as the simplest model for understanding some of the mechanisms in turbulent transport in atmospheric and oceanic flows.

In the seminal work by Batchelor [1] and Kraichnan [14, 15] a spectral approach, local in wavenumber space, was adopted to deduce a k^{-3} scaling of the energy spectrum in the inertial range, which is dominated by nonlinear transport and is not directly affected by viscosity. According to their theory, two-dimensional turbulence is characterized by an inverse energy cascade primarily towards larger scales, a property first noted by Onsager [16], and a direct enstrophy cascade primarily towards smaller scales [7, 12]. There is increasing numerical evidence however that the actual spectrum is significantly steeper than the celebrated Batchelor-Kraichnan spectrum, see for example [2, 4, 19]. It has been argued that vortex dynamics and coherent structures, which are local in physical space and therefore non-local in spectral space, are responsible for the deviations from the Batchelor-Kraichnan theory. Most of the energy in a turbulent flow is contained in vortices which spontaneously form out of initial random fields.

In a series of papers [2, 3, 5, 18] several scaling theories have been proposed which take into account the dynamical importance of vortices. In [2, 3] the algebraic scaling of the energy spectrum was linked to an emerging distribution of vortices with area A having an algebraic number density $n(A) \sim A^{-p}$. (The area A of a vortex may be defined as the size of a contiguous region having vorticity e.g. exceeding the r.m.s. vorticity over the domain.) The exponent p was determined by fitting to numerical simulations. A temporal scaling of the vortex number density was proposed in [5, 18]. Assuming that, in addition to energy, the maximal vorticity during vortex interactions is conserved, dimensional arguments lead to $n \sim t^{-\xi}$. The analysis however assumes vortices of one particular size, and does not predict the value of the scaling exponent ξ. Here we present a model which unifies the spatial and temporal scaling theories and moreover, determines the vortex number density as $n(A) \sim t^{-2/3}/A$ on using self-similarity. Our theory is supported by high-resolution numerical simulations.

Following [3] we write the total conserved enstrophy per unit area as

$$Q = \int_0^\infty \Omega(k)\, dk = \int_0^\infty k^2 \mathcal{E}(k)\, dk \ , \tag{1}$$

where $\Omega(k)$ and $\mathcal{E}(k)$ are the enstrophy and energy spectra at wavenumber k. Considering a population of vortices with a vortex number density $n(A)$ of vortices with area A we write

$$Q_v = \frac{1}{2A_s} \int_0^{A_s} \omega_v^2 A n(A)\, dA \ , \tag{2}$$

where Q_v is the part of Q associated with the vortices, ω_v is the vorticity magnitude, and A_s is an arbitrary domain size. We now assume that most of the energy is contained within the vortices, and that the vorticity of each vortex ω_v does not vary for vortices with different areas A. Identifying $A \sim k^{-2}$ so that $dA \sim k^{-3}\, dk$, comparison of (1) and (2) gives the energy spectrum

$$\mathcal{E}(k) \sim \omega_v^2 A_s^{-1} n(A) k^{-7} \ . \tag{3}$$

The vortex number density is assumed to be of the form $n(A) \sim A^{-p}$ implying $\mathcal{E} \sim k^{-7+2p}$. Up to here our analysis is equivalent to the one performed in [3]. Therein p is determined by numerically fitting the energy spectrum (3) for a prescribed vortex distribution. Note that the classical Batchelor-Kraichnan spectrum is recovered for $p = 2$. In the following however, we show that only $n(A) \sim A^{-1}$ allows for a self-similar vortex distribution. The energy spectrum associated with a self-similar vortex distribution then scales as

$$\mathcal{E}(k) \sim k^{-5} \ . \tag{4}$$

To study scale-invariance of a vortex distribution we first define the area fraction of an arbitrary area A_s occupied by vortices

$$f_v = \frac{1}{A_s} \int_0^{A_{\max}} A n(A)\, dA \ .$$

Here $A_{\max}$ is the maximal vortex size in A_s. Each vortex with area A occupies a *zone* the area of which is A/f_v. The sum of all zones is equal to the total area A_s. Now consider a subdomain $A_0 < A_{\max}$ which is populated by non-overlapping vortices with areas $A \leq A_0$. Arguably, these vortices typically populate an area $A_{\rm rem}$ which is not already occupied by zones of vortices with area $A > A_0$ since strong shear surrounding these vortices would tear apart smaller vortices nearby, as explicitly demonstrated in [9]. This left-over area is just

$$A_{\rm rem} = \frac{1}{f_v} \int_0^{A_0} A n(A)\, dA \ .$$

Self-similarity means that the ratio $A_0/A_{\rm rem}$ must be independent of the subdomain A_0. The only choice for $n(A)$ with this property is

$$n(A) = \frac{c}{A} \ . \tag{5}$$

Note that for such a density the number of vortices between μA_0 and A_0, $\mu \ll 1$, is

$$N_v = \int_{\mu A_0}^{A_0} \frac{c}{A} dA = c \ln \mu^{-1} \ , \tag{6}$$

which is independent of the subdomain A_0, again illustrating the self-similarity associated with the special form of the vortex number density (5).

Next we study the temporal behaviour of the number density $n(A,t) = c(t)/A$. We generalize the approach of [5]; instead of a gas of equal-sized vortices, we consider a distribution of vortices with a maximum vortex radius $a(t) \sim \sqrt{A_{\rm max}}$. The total energy scales as

$$E = \frac{1}{2A_s} \int |\mathbf{u}|^2 \, dxdy \sim \frac{1}{2A_s} \int_0^{A_{\rm max}} \omega_v^2 A^2 n(A) \, dA \sim c a^4$$

where we again assume that ω_v does not vary with the vortex area A. Conservation of energy then implies $c \sim a^{-4}$. The scaling of the enstrophy and the area fraction can then be obtained as

$$Q_v(t) \sim a^{-2} \qquad \text{and} \qquad f_v(t) \sim a^{-2} \ . \tag{7}$$

The temporal behaviour of the maximal vortex radius $a(t)$ is determined by the rate of enstrophy transfer from vortices to filaments dQ_v/dt. This transfer occurs through destructive vortex interactions. Vortex interactions typically involve three vortices, e.g. two vortices brought together by a third. The simplest model of this, and statistically the most common situation, is the interaction of a vortex dipole with a third, isolated vortex. The dynamical importance of this mechanism for enstrophy transfer has been known for some time and has been verified for a dilute population of vortices in [10]. This interaction can be destructive and results in the transfer of enstrophy from the vortex population to small-scale filaments. Self-similarity now implies that the enstrophy at any scale, $\omega_v^2 A n(A) dA$, decays at a rate which is independent of scale. We therefore equate

$$\frac{dQ_v}{dt} \sim -p_{\rm col} \frac{Q_v}{T_{\rm int}} \ , \tag{8}$$

where $p_{\rm col}$ is the collision probability of a dipole with smaller vortices and $T_{\rm int}$ is the time for a dipole to travel a characteristic inter-vortex distance $r(t)$. Since the collision probability is proportional to the vortex number density we have $p_{\rm col} \sim c \sim a^{-4}$. Using (6) the characteristic inter-vortex distance $r(t)$ of vortices with sizes between μA_0 and A_0 is given by

$$r \sim (A_0/N_v)^{1/2} \sim (A_0/c)^{1/2} \sim A_0^{1/2} a^2 \ . \tag{9}$$

The typical time $T_{\rm int}$, which measures the time a dipole of area A_0 and width proportional to $A_0^{1/2}$ travels a distance r, can be estimated as

$$T_{\rm int} = \frac{r}{U_{\rm dip}} \ , \quad \text{with} \quad U_{\rm dip} = \frac{\omega_v A_0}{A_0^{1/2}} \sim A_0^{1/2} \tag{10}$$

being a characteristic dipole velocity. Note this implies $T_{\rm int} \sim a^2$, independent of A_0 as required by self-similarity. Substituting (9)–(10) into (8) we obtain a differential equation for the size of the largest vortices

$$\frac{1}{a^3}\frac{da}{dt} \sim \frac{1}{a^8} \quad \text{which implies} \quad a(t) \sim t^{1/6} \ .$$

Together with (5) this uniquely determines the vortex number density

$$n(A,t) \sim \frac{t^{-2/3}}{A} \ . \tag{11}$$

Furthermore via (7) we can determine the temporal scaling behaviour of the enstrophy $Q_v(t)$ and the area fraction $f_v(t)$ as

$$Q_v(t) \sim t^{-1/3} \qquad \text{and} \qquad f_v(t) \sim t^{-1/3} \ . \tag{12}$$

We note that the temporal decay rate ξ of the vortex number density of $\xi = 2/3$ is consistent with previous numerical estimates [3–6, 18]. Our approach of considering a self-similar vortex distribution allows a unique determination of the spatial and temporal scaling behaviour of the vortex density $n(A,t)$ and subsequently of the total vortex enstrophy $Q_v(t)$ and area fraction occupied by vortices $f_v(t)$.

To corroborate our model, ensemble statistics were determined from 20 high-resolution numerical simulations carried out using the CASL algorithm, a hybrid contour dynamics/spectral method capable of accurately modelling an especially wide range of scales [8], with great care taken to minimise the numerical dissipation over long integration times (details will be published elsewhere). Each simulation began with a random-phased vorticity distribution with energy spectrum $\mathcal{E}(k) = \alpha k^3 \exp(-2k^2/k_0^2)$, with $k_0 = 32$ and α chosen so that $E = 1/2$. Then $Q(0) = k_0^2/2$. In time, numerical dissipation strongly reduces Q, whereas E remains conserved to within a few percent, consistent with previous studies. Importantly, the numerical dissipation here acts only on thin vorticity filaments, not on sharp vorticity gradients, thereby preserving many small-scale vortices.

Each of the 20 simulations differed only in a random number seed. Each was run for 160 'eddy rotation periods' $T_{\rm eddy} \equiv 4\pi/\omega_{\rm rms}(0)$, where $\omega_{\rm rms}(0) = \sqrt{2Q(0)} = k_0$ is the initial r.m.s.

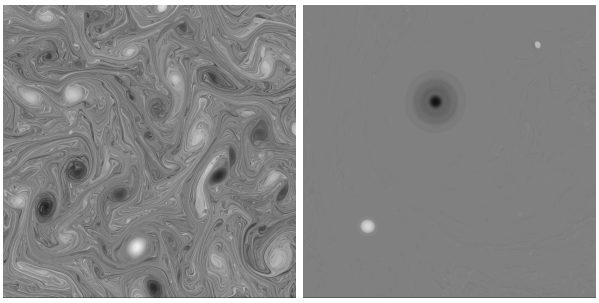

FIG. 1: Vorticity field at $t = 4$ (left) and $t = 160$ (right) in one representative simulation. A linear greyscale is used, with the highest positive vorticity being white. Only $1/16$th of the domain is shown.

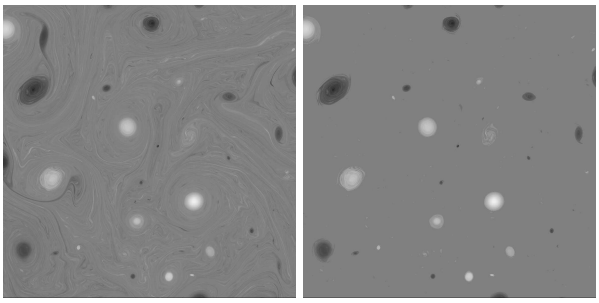

FIG. 2: Full vorticity field $\omega(\mathbf{x}, t = 16)$ (left) and its corresponding coherent part (right). Only $1/16$th of the domain is shown.

vorticity. Time is measured in units of $T_{\rm eddy}$. The most intense vortices rotate 4 to 5 times in one such unit of time.

The simulations use a basic 512×512 'inversion grid' for computing the velocity field, while a much finer resolution is used to represent the vorticity, as contours, down to scales of a twentieth of the basic grid size [8]. This results in an accurate representation of the vorticity dynamics down to the scale of numerical dissipation. The vorticity evolution in one representative simulation at early and late times is shown in figure 1.

To test the above scaling theory, coherent vortices were identified by computing contiguous regions of vorticity with $|\omega| > \omega_{\rm rms}(t)$, and aspect ratio $\lambda < 2 + \sqrt{3} \approx 3.73$. Doubling or halving these thresholds has little effect on the following results. In figure 2 we show the full vorticity field of one representative simulation at 16 eddy rotation periods and its corresponding coherent part as defined above.

The vortex area A and the mean vorticity ω_v associated with the coherent vortices can then be calculated as $A = \Gamma^2/\eta$ and $\omega_v = \eta/\Gamma$ with enstrophy of a coherent vortex η and circulation of a

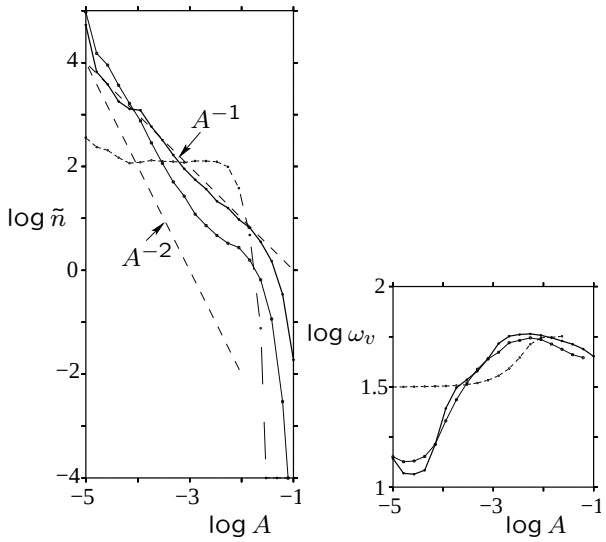

FIG. 3: Ensemble averaged normalised number density (left) and mean vorticity ω_v (right) versus area, in logarithmic scales; $t = 0$ is shown by a dashed line with diamonds, $20 \leq t \leq 30$ (averaged) is shown by a thin line with squares, and $100 \leq t \leq 160$ is shown by a bold line with triangles.

coherent vortex Γ. The vortex number density $n(A)$ and the mean vorticity ω_v are subsequently estimated by averaging over 20 logarithmically spaced bins between $A = 10^{-5}$ and $A = 10^{-1}$. The data were further ensemble averaged over the 20 realizations and time-averaged.

The normalised number density $\widetilde{n} \equiv n(A)/N_v$ is shown in figure 3 (left) time-averaged over several intervals. The late time density clearly scales as $n(A) \sim 1/A$ over 3 decades in area, consistent with the prediction of our self-similar theory. On the right in figure 3, we show $\omega_v(A)$ over the same time intervals. There is no systematic dependence on A, and ω_v^2 varies by only one order of magnitude over four orders of magnitude in A, and much less than this for $-4 < \log(A) < -1$, where arguably the flow is better resolved. This dependence on A is extremely weak, justifying the assumption $\omega_v \approx$ constant.

In figure 4, the enstrophy spectrum $\Omega(k)$, time averaged over the interval of 100–160 eddy rotation periods (thin line), is compared with its coherent part obtained from retaining only the coherent vortices. Figure 4 clearly illustrates that the steeper-than-Batchelor-Kraichnan scaling of the spectra at high-wavenumbers is associated with the presence of vortices, and the shallow part can be attributed to incoherent, predominantly filamentary vorticity. In time (not shown), this incoherent k^{-1} tail is swept to ever higher k, leaving behind a widening steeper spectrum associated with the coherent vortices. This steeper spectrum has a slope close to k^{-3}, corresponding to a $1/A$

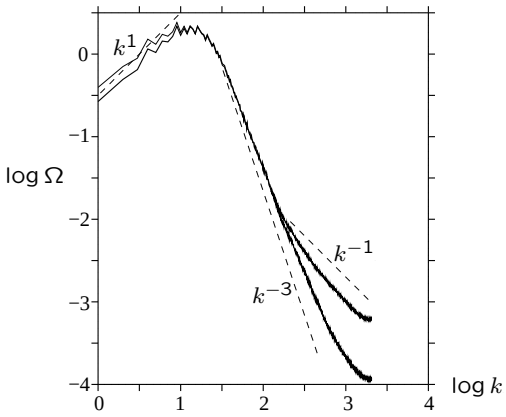

FIG. 4: Ensemble and time-averaged ($100 \leq t \leq 160$) enstrophy spectrum (thin line) and its coherent counterpart (bold line) versus wavenumber k, in logarithmic scales. Various slopes are indicated.

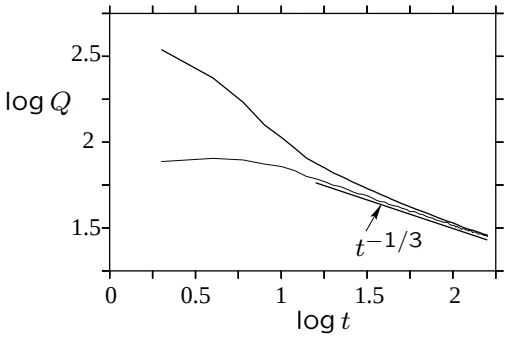

FIG. 5: Temporal decay of total (resolved) enstrophy $Q(t)$ (top curve) and coherent vortex enstrophy $Q_v(t)$ (bottom curve), in logarithmic scales.

distribution of vortices. The actual slope is slightly shallower, possibly due to the contribution of vorticity discontinuities at the coherent vortex edges (an artifact of our vortex identification method). In the corresponding energy spectrum $\mathcal{E}(k) = \Omega(k)/k^2$, we may therefore associate the steep k^{-5}-part of the energy spectrum with coherent vortices and the shallow k^{-3} part with filaments.

We turn finally to the temporal decay. Figure 5 shows the decay of total enstrophy $Q(t)$ [20] and its coherent part $Q_v(t)$ (ensemble averaged), using logarithmic scales (similar results have been found for the area fraction f_v). The decay of $Q_v(t)$ is not a numerical artifact, but a genuine feature of the turbulent flow evolution. This decay is the result of vortex interactions, generating incoherent filamentary debris which cascade to ever finer scales. At late times, both curves approach a $t^{-1/3}$ decay, consistent with the prediction of our theory and with previous numerical

results [4, 6, 18]. Most remarkably, $Q_v(t)$ closely follows a $t^{-1/3}$ decay for the last 90% of the flow evolution, i.e. coherent vortex interactions dominate the long term behaviour of enstrophy — crucial for our self-similarity assumption.

In summary, this paper presents a scaling theory for unforced inviscid two-dimensional turbulence based on a self-similar vortex distribution. The theory predicts a steeper than Batchelor-Kraichnan scaling for the energy spectrum at large wavenumbers with $\mathcal{E}(k) \sim k^{-5}$ due to coherent vortices, and a temporal scaling of vortex enstrophy $Q_v(t) \sim t^{-1/3}$. The model is consistent with and extends previous spatial [2, 3] and temporal [5, 18] scaling theories and numerical simulations [3–6, 18]. This is arguably the first consistent turbulence model which deduces all free parameters from just a few assumptions without any empirical fitting to data. The model is confirmed by high-resolution CASL simulations carried out to very long times. In particular, the simulations and the associated vortex ensemble statistics underscore the importance of vortices for the steepening of the energy spectra. The decay of coherent enstrophy implies that essentially all of the enstrophy transfers from vortices to filaments, via vortex interactions, as $t \to \infty$ [11, 17]. The enstrophy accumulates within a k^{-1} filamentary tail which spreads to $k \to \infty$. In a subsequent paper [13], we discuss the implications of this enstrophy cascade. One key result however can be immediately deduced: the $t^{1/6}$ growth of the largest vortices predicted here implies a correspondingly slow, but inevitable, inverse energy cascade.

GAG is partly supported by ARC grant DP0452147.

[1] G. K. Batchelor, Phys. Fluids **12**, 233 (1969).

[2] R. Benzi, S. Patarnello and P. Santangelo, J. Phys. A **21**, 1221 (1988).

[3] R. Benzi, M. Colella, M. Briscolini and P. Santangelo, Phys. Fluids **4**, 1036 (1992).

[4] A. Bracco, J. C. McWilliams, G. Murante, A. Provenzale and J. B. Weiss, Phys. Fluids **12**, 2931 (2000).

[5] G. F. Carnevale, J. C. McWilliams, Y. Pomeau, J. B. Weiss and W. R. Young, Phys. Rev. Lett. **66**, 2735 (1991).

[6] H. J. H. Clercx, S. R. Maassen and G. J. F. van Heijst, Phys. Fluids **11**, 611 (1999).

[7] P. A. Davidson, *Turbulence: An Introduction for Scientists and Engineers.* (Oxford Univ. Press, 2004).

[8] D. G. Dritschel and M. H. P. Ambaum, Quart. J. Roy. Meteorol. Soc. **123**, 1097 (1997).

[9] D. G. Dritschel and D. W. Waugh, Phys. Fluids **4**, 1737 (1992).

[10] D. G. Dritschel and N. J. Zabusky, Phys. Fluids **8**, 1252 (1996).

[11] D. G. Dritschel, C. V. Tran and R. K. Scott, J. Fluid Mech. **591**, 379 (2007).

[12] U. Frisch *Turbulence: the Legacy of A. N. Kolmogorov.* (Cambridge Univ. Press, 1995).

[13] D. G. Dritschel, R. K. Scott, C. Macaskill, G. A. Gottwald and C. V. Tran, in preparation.

[14] R. H. Kraichnan, Phys. Fluids **10**, 1417 (1967).

[15] R. H. Kraichnan, J. Fluid Mech. **47**, 525 (1971).

[16] L. Onsager, Nuovo Cimento **6**, 279 (1949).

[17] D.G. Dritschel and C. V. Tran, J. Fluid Mech. **559**, 107 (2006).

[18] J. B. Weiss and J. C. McWilliams, Phys. Fluids **5**, 608 (1993).

[19] J. C. McWilliams, J. Fluid Mech. **146**, 21 (1984).

[20] enstrophy decays only because of the finite numerical resolution; for any finite time the enstrophy dissipation vanishes in the inviscid limit [11, 17].